Molecular and Crystal Deformation in Poly(aryl ether ether ketone) Fibers

Kenny Kong,[†] Richard J. Davies,[‡] Robert J. Young,*[,†] and Stephen J. Eichhorn[†]

Materials Science Centre, School of Materials, Grosvenor Street, University of Manchester, Manchester M1 7HS, U.K., and European Synchrotron Radiation Facility, B.P. 220, F-38043, Grenoble Cedex, France

Received June 22, 2008; Revised Manuscript Received August 13, 2008

ABSTRACT: The molecular and crystal deformation of single fibers of PEEK (poly(aryl ether ether ketone)) has been followed using a combination of Raman spectroscopy and X-ray diffraction. The molecular orientation of the fibers is characterized using polarized Raman spectroscopy, and it is shown that the high degree of molecular orientation is in agreement with crystal orientation revealed by X-ray diffraction. By using a submicron (500 nm) X-ray beam size to map across a single fiber diameter, it is shown that there is no difference between the orientation of the skin of the fiber and the core. Upon deforming the fibers in tension, Raman spectroscopy reveals that a number of bands, particularly the 1147 cm^{-1} (C−O−C stretch) and the 1610 cm^{-1} (phenylene ring stretch) modes, shift toward a lower wavenumber position, which is known to be indicative of direct molecular deformation. It is shown that these shifts in the Raman band peak positions are nonlinear with strain and stress and that they follow the form of the stress−strain curves obtained for the fibers. Two changes in slope are noted in the shifts of these peaks, which coincide with the yield points in the stress−strain curve. The magnitude of the initial slope of the shift in the 1147 and 1610 cm^{-1} bands with tensile deformation is shown to be close to that reported for both cellulose and other *p*-phenylene ring based fibers. Using X-ray diffraction, it is also shown that the crystals undergo deformation during fiber stretching. The crystal modulus of the fibers is reported and shown to be in agreement with previously published data. In addition, it is shown that the uniform skin−core morphology is maintained during deformation.

1. Introduction

Poly(aryl ether ether ketone), PEEK, is a thermoplastic polymer which has been used widely for engineering applications and composite materials due to its highly desirable properties.[1−3] The chemical structure was first reported in the literature in 1981,[4] as shown in Figure 1, and the morphological structure was first described by Blundell and Osborn in 1983.[5] It can be seen from Figure 1 that the repeat unit comprises three *p*-phenylene rings connected by C−O−C linkages, which forms the backbone structure of the polymer.

The first Raman spectroscopic study of PEEK was reported in 1986 by Louden,[6] who assigned Raman peaks to the particular molecular structure of PEEK and also correlated their relative intensities with crystallinity.[6] These results were independently confirmed by Everall et al.[7] It has also been shown, using FT-Raman spectroscopy, that the intensity of the C−O−C stretching mode in PEEK increases with increasing temperature.[8,9] Residual stresses in PEEK−carbon fiber composites have also been determined using Raman spectroscopy[2,3] although no reports, to the authors' knowledge, exist on measuring molecular deformation in single PEEK fibers. Raman spectroscopy has been used extensively to monitor molecular deformation in a large number of polymeric fibers.[10] The technique relies on the measurement of a shift in the peak position of a Raman band with respect to external deformation and was first discovered for polymeric fibers by Mitra et al.[11] and has subsequently been used for a wide variety of other fibrous materials.[10]

The crystal deformation and orientation of polymeric fibers using X-ray diffraction from a synchrotron source has been successfully applied to single polymeric rigid-rod fibers, such as poly(*p*-phenylene benzobisoxazole)[12−15] and cellulose fibers.[16] In terms of X-ray diffraction studies of PEEK, Rueda et al. conducted a study using a die drawn bar of material and reported an orthorhombic unit cell structure with dimensions $a = 7.75$ Å, $b = 5.89$ Å, and $c = 9.88$ Å.[17] A later study conducted by Frantini et al. reported a crystal structure of PEEK obtained from a die drawn film of material, which had similar dimensions of $a = 7.83$ Å, $b = 5.94$ Å, and $c = 9.86$ Å.[18] The crystal modulus of PEEK, obtained from a deformed film of material, has been reported to be 31 GPa, using the shift of the (002) reflection to record crystal strain.[19] However, an X-ray diffraction study of the crystal deformation of a single PEEK fiber has not been previously reported. A study by Voice et al.[20] reported the change in crystal orientation associated with a change in the draw ratio; an increase in this parameter accompanied the increase in the orientation.

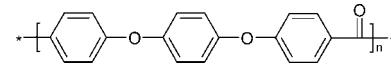

Figure 1. Repeat unit of PEEK (poly(aryl ether ether ketone)).

The purpose of the present investigation is the report on the molecular and crystal deformation of highly aligned PEEK fibers. These fibers may have applications as reinforcements in all-polymer thermoplastic composites produced by hot compaction,[21] which have been recently reported.[22−25] Currently these fibers have their main uses as a conveyer belt material, a filter material, and tennis and badminton racquet strings.[26]

2. Experimental Section

2.1. Materials. Single fibers of PEEK were obtained from Zyex, UK. These fibers were studied as-supplied and came with no presurface treatments. Their diameters were found to be 23.4 ± 0.3 μm using scanning electron microscopy.

2.2. Sample Preparation. PEEK fiber single filaments were secured using cold-curing epoxy resin (Araldite) to 50 mm gauge length testing cards, as has previously been described for other

* Corresponding author: Tel +44-161-306-3551; Fax +44-161-306-3586; e-mail robert.young@manchester.ac.uk.
[†] University of Manchester.
[‡] European Synchrotron Radiation Facility.

10.1021/ma801402w CCC: $40.75
Published on Web 10/04/2008

polymer fiber samples.[12−16] These samples were then used to analyze both the structure and the mechanical properties of the fibers.

2.3. Structural Characterization of PEEK Fibers. *2.3.1. Raman Spectroscopy and Orientation.* A Renishaw system 2000 Raman spectrometer coupled to an Olympus microscope was used to monitor fiber deformation. A near-IR laser ($\lambda = 830$ nm), focused to a spot size of about 2 μm on the surface of the sample using a $\times$ 50 lens, was used to excite Raman scattering from the fibers. Previous Raman spectroscopic studies of PEEK, using laser wavelengths other than near-IR sources, have typically produced spectra dominated by fluorescence[2,3] which has made it difficult to obtain resolvable spectral peaks. In order to obtain clear Raman spectra a 60 s (10 s and 6 accumulations) exposure time was used. The monochromatic light from the laser was polarized, and the analyzer was set to record both parallel and perpendicularly polarized light from the scattered radiation. A half-wave plate was used to rotate the polarization of the incoming radiation by 90°.

2.3.2. X-ray Diffraction and Orientation. The crystal structure and orientation analysis of the fibers was carried out at the European Synchrotron Radiation Facility (ESRF) on beamline ID13. The wavelength of the radiation used was 0.98 Å with a specimen-to-camera distance of ~147 mm. Images of the X-ray diffraction patterns were recorded on a 1024 × 1024 pixel CCD camera, each pixel having an area of 157.9 × 157.9 μm^2. Fit2D software (version 12.077) was used to analyze the diffraction patterns.[27,28] In order to obtain clear diffraction patterns, an exposure time of 10 s was used. The skin−core orientation distribution of the fibers was determined by scanning across a complete fiber width using a spatial step size of 500 nm (= beam size), recording a diffraction pattern at each point.

The value of the orientation parameter $\langle \sin^2 \theta \rangle$, which gives an indication of the degree of crystal orientation, was determined by using the equation[29]

$$\langle \sin^2 \theta \rangle = \frac{\int_0^{\pi/2} \rho(\theta) \sin^3 \theta \, d\theta}{\int_0^{\pi/2} \rho(\theta) \sin \theta \, d\theta} \quad (1)$$

where $\rho(\theta)$ is the azimuthal distribution of the (200) reflection. For perfect crystal orientation the orientation parameter is equal to zero. This orientation parameter has been used instead of the more widely employed Hermans orientation distribution function as it can be related directly to the mechanical properties of high-performance fibers.[29]

2.4. Mechanical Properties. *2.4.1. Mechanical Properties of Single Fibers.* The mechanical properties of the single fibers were determined by mounting single filaments on the testing cards, as described earlier. These samples were then mounted into the jaws of an Instron-1121 universal tensile testing machine, with a 1 N load cell. The sides of the tensile testing card were then burnt away using an artist's pyrography machine. The cross-head speed was set to give a strain rate of 0.166% s^{-1}. Twenty specimens were deformed in tension for statistical reliability. All samples were tested under controlled conditions of 23 ± 1 °C and 50 ± 5% relative humidity. In order to determine the fiber stress, the diameter of a single fiber was obtained using a magnification calibrated Philips FEG scanning electron microscope (SEM) with an accelerating voltage of 5.0 kV. The diameters of a number of fibers (30) were determined using image analysis software, and a mean value of the cross-sectional area was calculated, assuming a circular cross section. The load values obtained from the Instron tensile testing machine were then converted to engineering stress using this fixed value of the cross-sectional area.

2.4.2. Determination of Molecular Deformation Using Raman Spectroscopy. The Renishaw system 2000 Raman spectrometer system, with an 830 nm laser, was also used to record the molecular deformation. Single fibers were deformed under the microscope of the Raman spectrometer using a customized loading rig. A 5 N load cell coupled to a transducer was used to record the load on the fibers, which was later converted to fiber stress using the cross-sectional area. A parallel−parallel polarization configuration was used to excite and record the scattered Raman intensities from the sample. An exposure time of 60 s (10 s and 6 accumulations) was again used. The samples were deformed in tension using strain increments of 0.2%, and Raman spectra were collected in the range 1100−1700 cm^{-1}. These spectra were fitted using mixed Gaussian and Lorentzian functions, based on an algorithm developed by Marquardt,[30] in order to determine the peak positions as a function of fiber deformation. In order to find the position of the 1147 cm^{-1} peak, only a single Gaussian/Lorentzian function was required, whereas multiple peak fitting was required to find the position of the 1610 cm^{-1} band.

2.4.3. Determination of Crystal Deformation and Orientation Changes Using X-ray Diffraction. The same experimental setup, as described earlier, was used in order to follow the deformation of the crystals in the fibers. Single fibers, mounted on fiber testing cards, were attached to a customized loading rig and deformed in tension. A series of diffraction patterns were obtained across a fiber width, at each loading stage, using a spatial step size of 500 nm. Approximately 60 diffraction patterns, across a fiber diameter, were obtained for each loading level. All diffraction patterns were analyzed to determine both the *c*-spacing and orientation function $\langle \sin^2 \theta \rangle$ using the Fit2D software.[27,28] The *c*-spacing was determined from the central position of the meridional (002) reflection using the equation

$$c\text{-spacing} = \frac{n\lambda}{\sin(\tan^{-1}(x/r))} \quad (2)$$

where λ is the radiation wavelength, n is the order of the reflection, x is the vertical height of the (002) reflection on the recorded diffraction pattern, and r is the sample-to-CCD camera distance.[31] Using the initial measurement of *c*-spacing (c_0) and subsequent measurements (c), it is possible to determine the crystal strain (ε_c) using the equation

$$\varepsilon_c = \frac{c - c_0}{c_0} \quad (3)$$

The orientation function $\langle \sin^2 \theta \rangle$ was found by using eq 1 and was determined spatially across a single fiber, at different levels of tensile deformation.

3. Results and Discussion

3.1. Structural Characterization of PEEK Fibers. Typical Raman spectra for all four polarization configurations, obtained from a single PEEK fiber, are shown in Figure 2. These data indicate a typical PEEK structure, as seen independently using unpolarized Raman spectroscopy.[6,32] The intensity of the 1147 cm^{-1} band, associated with the backbone C−O−C bonds of the PEEK structure,[6] is much smaller in the perpendicular−perpendicular polarization configuration than the parallel−parallel configuration. This suggests that the PEEK molecular chains are oriented close to the fiber axis. In addition to this, the 1610 cm^{-1} band associated with the *p*-phenylene ring structure[6] is almost completely absent in the perpendicular−perpendicular orientation, again suggesting a high degree of molecular orientation. Raman spectra obtained using perpendicular−parallel and parallel−perpendicular polarization configurations are also shown in Figure 2. Both these Raman spectra appear similar in profile, as would be expected for a uniaxially oriented sample due to fiber symmetry.

An X-ray diffraction pattern obtained from a single PEEK fiber is shown in Figure 3. The azimuthal intensity distribution of the (200) reflection was used to obtain the orientation parameter for the fiber as a function of the position across the fiber width. These data show, for an undeformed fiber, that there are no significant differences between the orientation parameters

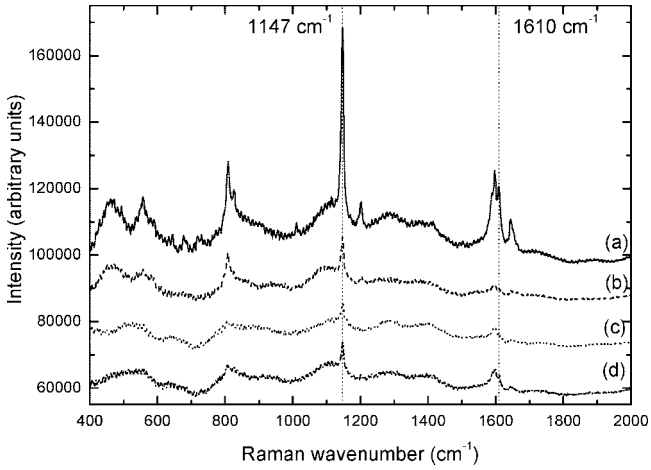

Figure 2. Raman spectra obtained from single PEEK fibers using (a) parallel−parallel, (b) perpendicular−perpendicular, (c) perpendicular−parallel, and (d) parallel−perpendicular polarization configurations. Dotted lines indicate the positions of the 1147 and 1610 cm^{-1} Raman bands.

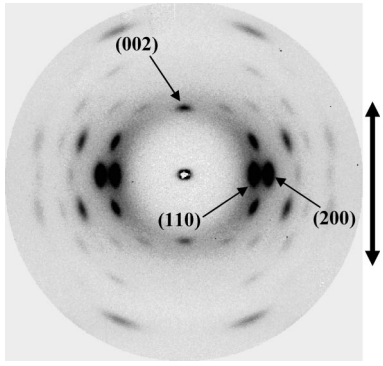

Figure 3. X-ray diffraction pattern obtained from a single PEEK fiber with the (002), (110), and (200) reflections labeled. The arrow indicates the fiber axis.

obtained from both the skin and the core (see later). This result is similar to that observed for PBO fibers.[15] This is, however, in contrast to regenerated cellulose fibers,[16,33,34] where large skin−core orientation differences have been observed.

3.2. Mechanical Properties of PEEK Fibers. The stress−strain curve for a single PEEK fiber is shown in Figure 4, with arrows indicating the position of two yield points at about 1.5% and 12% strain. These data indicate characteristically nonlinear stress−strain behavior. Double yield points have been previously observed for thermoplastic polymers such as polyethylene,[35,36] where the second yield point was attributed to permanent deformation and coincided with a necking of the sample. An initial yield point in the range 0.5−2%, due to a sequential plastic orientation mechanism, has been reported for a range of thermoplastic polymer fibers.[37] A summary of the PEEK fiber mechanical properties is given in Table 1. The values of the breaking strength and Young's modulus are slightly higher than values reported in the literature for PEEK films.[19] This is to be expected since it is likely that the molecular orientation of a fiber will be higher than for a film. It should be pointed out that these data were derived assuming that the cross-sectional area of the fibers does not change during deformation and so are not based on a true representation of the stress−strain behavior of the material, since nominal stress data are reported.

3.3. Analysis of the Micromechanical Deformation of PEEK Fibers Using Raman Spectroscopy. The central maximum of the 1147 cm^{-1} Raman band was found to shift

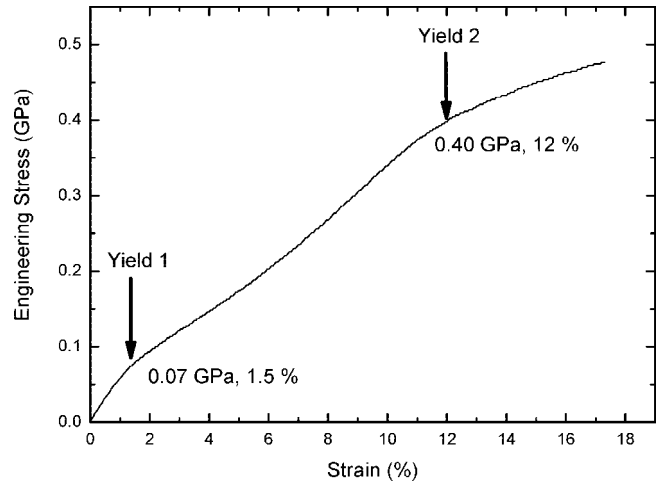

Figure 4. Stress−strain curve for a single PEEK fiber with arrows indicating the positions of yield points.

Table 1. Mechanical Properties of Single PEEK Fibers[a]

fiber diameter (μm)	Young's modulus (GPa)	breaking strength (GPa)	breaking elongation (%)
23.4 ± 0.3	7.37 ± 1.60	0.59 ± 0.18	16.5 ± 1.2

[a] All data quoted to 3 significant figures, and errors are standard deviations from the mean.

during tensile deformation. An example of this shift is shown in Figure 5a, which is thought to be indicative of the direct deformation of the C−O−C bonds within the polymer backbone.[2,3] The shifts in the peak position of this band with respect to fiber strain and stress are given in Figure 5b,c. The shift in both sets of data is nonlinear, reflecting the shape of the stress−strain curve. An inflection in these data is observed at 1.5% strain (Figure 5b) and ∼ 0.1−0.2 GPa stress (Figure 5c), which coincides roughly with the first yield point in the stress−strain curve for these fibers (cf. Figure 4 and the yield point at 1.5% strain). It is worth pointing out, however, that the rates of deformation applied during these two tests are likely to be different, a factor which may affect the position of the yield point in each case. A second change in the slope of these data is also noted at ∼12% strain. This inflection in these data also coincides with the second yield point in the stress−strain curve for these fibers (cf. Figure 4 and the yield point at 12% strain).

The shift rate with respect to strain for the 1147 cm^{-1} band and that observed for cellulose fibers (the 1095 cm^{-1}) are worth comparing, since both correspond to a C−O−C stretch mode. A direct comparison cannot be made, given that PEEK and cellulose have entirely different structures, and so the transfer of stress to the molecular structure will not be the same. Nevertheless, this value (−0.55 cm^{-1} $\%^{-1}$) is only slightly higher than that obtained for lyocell fibers (found to be in the range 0.16−0.43 cm^{-1} $\%^{-1}$)[38] but lower than a value (−1.08 cm^{-1} $\%^{-1}$) reported for a high modulus cellulose fiber (Bocell).[33] The initial shift rate with respect to stress before the yield point (−5.55 cm^{-1} GPa^{-1} in Figure 5c) is similar in magnitude to values previously reported for cellulose fibers,[39] which suggests a fundamental deformation mechanism within the molecular structures of these polymeric fibers. It is, however, worth noting that the modulus of PEEK is somewhat lower than most cellulose fibers and certainly the vast majority of high-performance *p*-phenylene based rigid-rod fibers. This low modulus may occur due to the fact that there are few chain−chain interactions within the structure. PEEK also possesses a nonlinear zigzag chain and, unlike cellulose, does

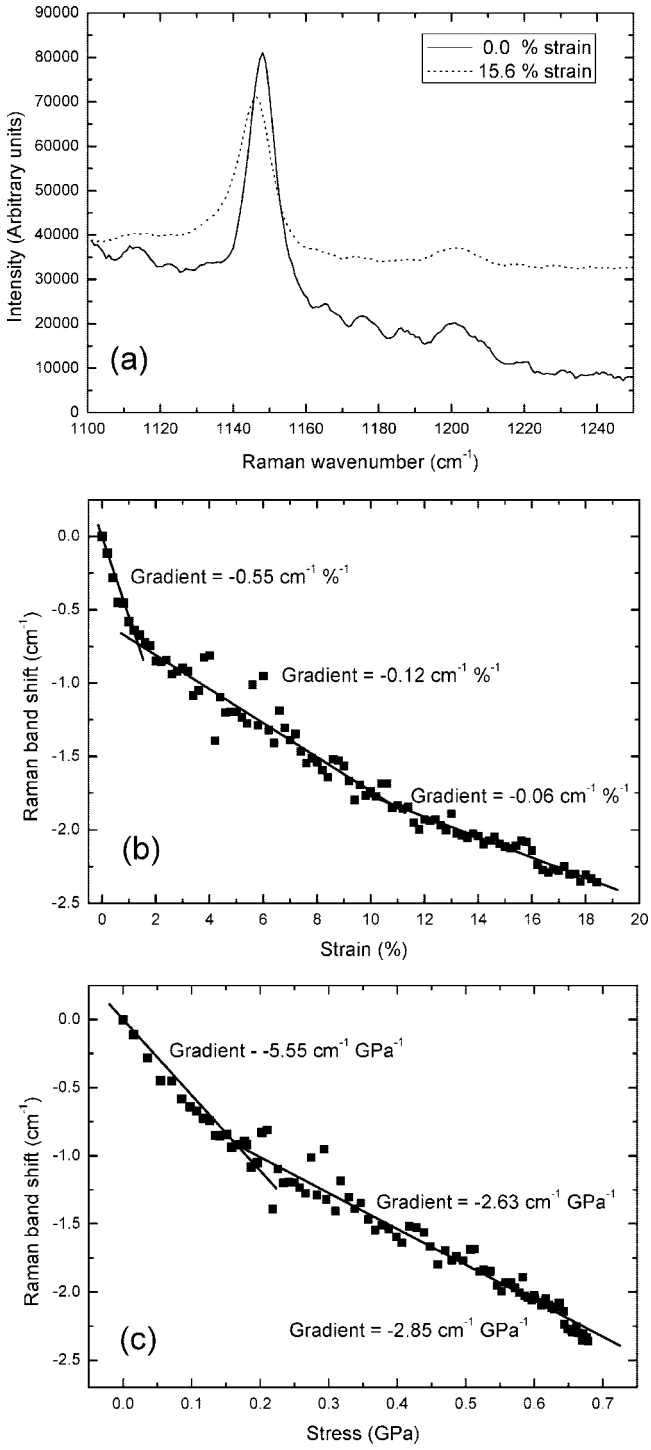

Figure 5. (a) Shifts in the 1147 cm^{-1} Raman band as a function of tensile deformation. Shifts in the central maximum position of the 1147 cm^{-1} band with (b) strain and (c) stress where the solid lines are linear fits to these data with the gradient of the fits indicated.

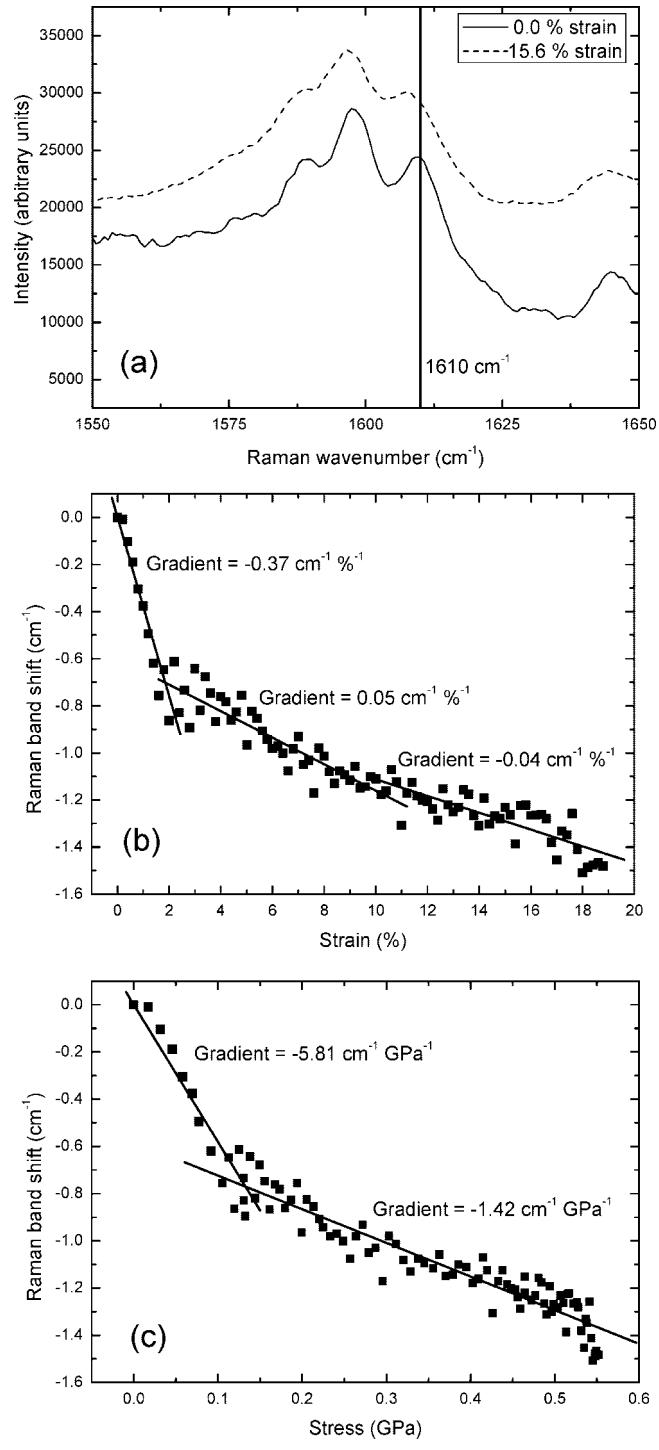

Figure 6. (a) Shifts in the 1610 cm^{-1} Raman band as a function of tensile deformation. Shifts in the central maximum position of the 1610 cm^{-1} band with (b) strain and (c) stress where the solid lines are linear fits to these data with the gradient of the fits indicated.

not have intrachain hydrogen bonding, which in the latter case gives rise to high stiffness.[40]

The 1610 cm^{-1} band, corresponding to the *p*-phenylene ring stretch mode,[14] was also observed to shift in position during tensile deformation (see Figure 6a). The shift rate in the peak position data with respect to strain for the 1610 cm^{-1} peak is much lower than those observed for rigid-rod fibers such as PBO (cf. -0.37 cm^{-1} in Figure 6b with $6-12$ cm^{-1} $\%^{-1}$). This is probably due to the difference in fiber moduli since the Raman band shift rate with respect to strain has been shown to be proportional to the fiber modulus;[10] PBO fibers have a much higher modulus (~300 GPa) than PEEK fibers (~7 GPa from Table 1). The band shift rate with respect to stress, however, for the PEEK fibers is marginally higher compared to values obtained for rigid-rod fibers (cf. -5.8 cm^{-1} GPa^{-1} from Figure 6c with -4.3 cm^{-1} GPa^{-1} for PBO[14] and -4.0 cm^{-1} GPa^{-1} for Kevlar fibers[41]). These differences could be due to the fact that the PEEK fibers possibly have a series-parallel microstructure of crystals and amorphous regions, whereas rigid rod fibers are known to possess series aggregate or uniform stress microstructures.[10] Two inflections in the 1610 cm^{-1} band shift data are observed, which coincide with the yield points in the

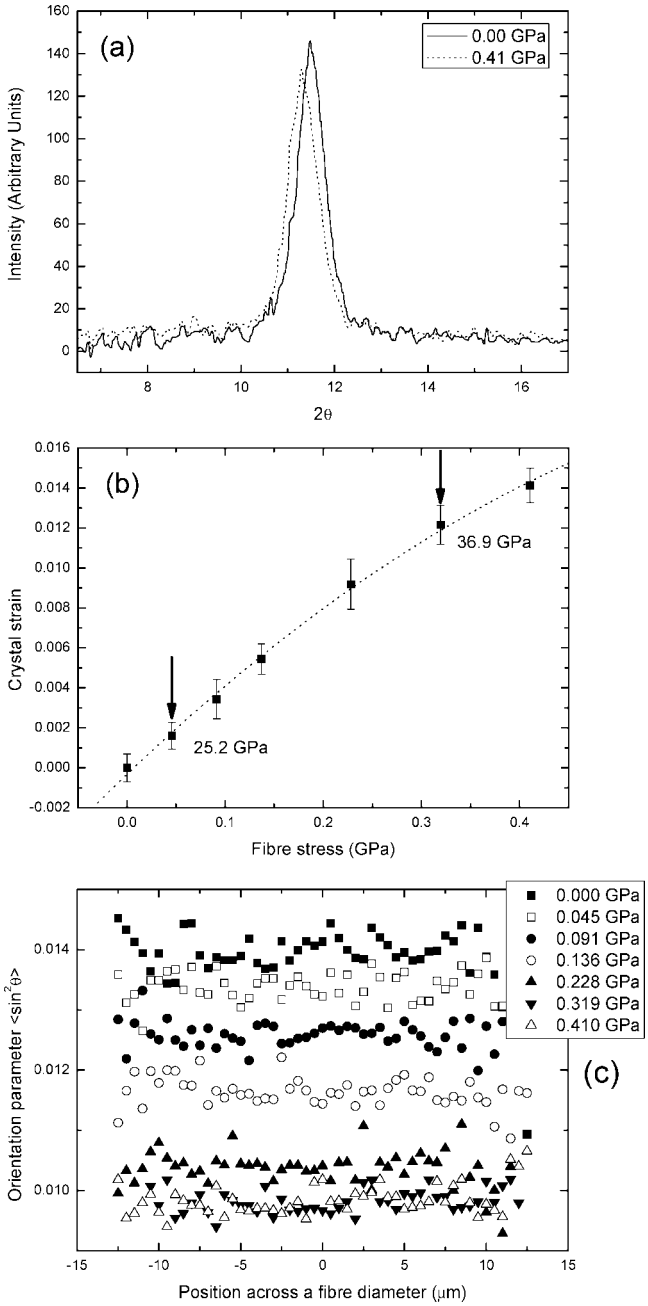

Figure 7. (a) Shift in the (002) reflection with fiber stress. (b) Crystal strain as a function of fiber stress. The dotted line is a polynomial fit for the eye only. (c) The orientation parameter $\langle \sin^2 \theta \rangle$ as a function of the position across a single PEEK fiber diameter at different levels of fiber stress.

stress−strain curve, as was seen for the 1147 cm^{-1} band. It is clear that the yield points in the stress−strain curve for PEEK fibers have some relationship to the molecular deformation processes that are occurring.

3.4. X-ray Diffraction Studies of Deformed PEEK Fibers. In order to understand the deformation mechanics of the crystalline fraction, X-ray diffraction was used to measure changes in the *c*-spacing during tensile deformation, as Raman spectroscopy does not discriminate crystalline and amorphous regions of a fiber structure.[10] The shift in the (002) reflection for a single PEEK fiber deformed in tension is shown in Figure 7a. This shift toward a lower 2θ angle (i.e., toward the center of the diffraction pattern shown in Figure 3) is indicative of direct deformation of the PEEK crystal, as has been observed

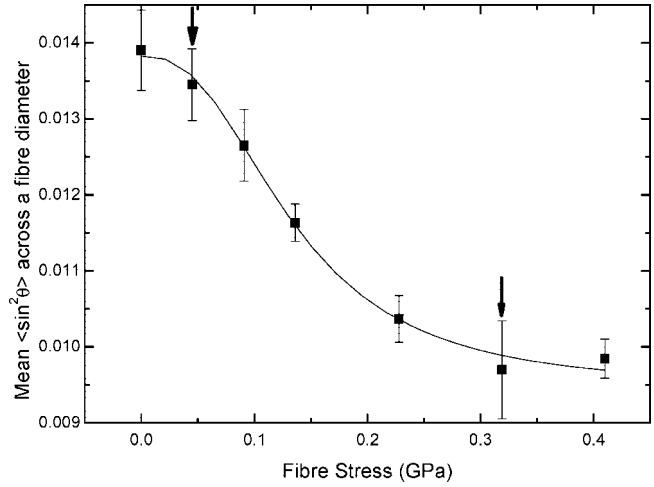

Figure 8. Mean orientation parameter $\langle \sin^2 \theta \rangle$ as a function of the fiber stress. The solid line is a guide for the eye only, and the arrows indicate the positions of the changes in the slope of the data.

before for a wide variety of polymeric fibers.[10] The mean crystal strain, as derived from eqs 2 and 3, is plotted as a function of the fiber stress in Figure 7b. These data indicate a nonlinear crystal stress−strain curve, a result which was also noted by Sakurada et al.[42] for poly(vinyl alcohol) and polyethylene fibers. The initial crystal modulus value of 25.2 GPa is much lower than a figure reported by Nishino et al.[19] of 71 GPa using the (008) reflection. Nishino et al.[19] also reported data for the (002) reflection, obtaining a value of 31 GPa, which is close to the value reported here. They attributed the differences between the crystal moduli obtained using different reflections to the fact that the Laue lattice factor changes as the crystal size increases.[19] An (008) reflection was not observed from the diffraction patterns obtained from the PEEK fibers, as we did not tilt our specimens, and so it was not possible to confirm the data of Nishino et al.[19] for this fiber type. The positions of two changes in the slope of these crystal strain data are reported in Figure 7, both of which coincide roughly with the yield points in the stress−strain curve.

The orientation parameter data as a function of the position across a fiber diameter with different levels of stress are shown in Figure 7c. It can be seen that the orientation parameter decreases with increasing stress, which suggests that crystals become oriented toward the fiber axis as tensile deformation proceeds. There is no change in the distribution of orientation of the crystals as deformation is applied to the fiber, and it is noted that $\langle \sin^2 \theta \rangle$ plateaus at the highest stress (>0.3 GPa), presumably reaching a structural limit. The data then superimpose, which coincides with the second yield point in the stress−strain curve. This is best illustrated by the data shown in Figure 8, where the mean orientation parameter across a single fiber diameter has been plotted as a function of fiber stress. These data show that at high stress the orientation parameter reaches a minimum, similar to the second yield point mechanism suggested for polyethylene.[35,36]

It was not possible to determine any changes in crystal size in the $\langle 001 \rangle$ direction during deformation since only one (002) reflection was available, and there are difficulties in accounting for instrumental broadening. The (002) reflection was found to broaden slightly during deformation indicating a possible reduction in crystallite size along $\langle 001 \rangle$.

4. Summary and Conclusions

The use of a combination of both Raman spectroscopy and microfocus X-ray diffraction to investigate the structure of and follow the molecular and crystal deformation in single fibers

of PEEK has been reported. Skin−core texture of the fibers, as revealed from X-ray diffraction studies, has also been investigated as a function of deformation. The stress−strain curve is found to be nonlinear, with three clear regions of deformation. The molecular and crystal deformation mechanisms that occur and give rise to these three regions, as revealed using combined Raman and X-ray diffraction, can be thus summarized:

Up to 1.5% strain there are large Raman band shift rates of a similar order of magnitude to high modulus fibers such as PBO, PPTA, and cellulose, accompanied by only a small change in the orientation parameter. Deformation in this region therefore appears to be dominated by chain stretching.

A yield point occurs at 1.5% strain, and then from 1.5 to 12% there is a reduced Raman band shift rate of both the 1147 and 1610 cm^{-1} peaks. It is thought that in this region deformation is dominated by the orientation of crystals toward the fiber axis, which can be seen clearly from Figure 8.

At 12% strain there is a second yield point, and after this there is a further reduction in the Raman band shift rates of both the 1147 and 1610 cm^{-1} peaks with respect to strain. There is no change in the Raman band shift rate of both bands with respect to stress, and the orientation does not change. It is therefore thought that molecular sliding occurs after this second yield point, and so no further orientation of crystals toward the fiber axis is possible.

Acknowledgment. The authors thank the EPSRC for funding this research (Grant Code: EP/C002164) and also Zyex Fibers for providing the PEEK fibers. The authors are also grateful to the European Synchrotron Radiation Facility (ESRF) for the award of beamtime. Dr. Jim Bennett (Manchester) is also gratefully acknowledged for assistance during the beamtime experiments. We also thank Dr. Andrew Hammersley for use of the Fit2D software application.

References and Notes

(1) Jones, D. P.; Leach, D. C.; Moore, D. R. *Polymer* **1985**, *26*, 1385–1393.
(2) Galiotis, C.; Melanitis, N.; Batchelder, D. N.; Robinson, I. M.; Peacock, J. A. *Composites* **1988**, *19* (4), 321–324.
(3) Young, R. J.; Day, R. J.; Zakikhani, M.; Robinson, I. M. *Compos. Sci. Technol.* **1989**, *34* (3), 243–258.
(4) Attwood, T. E.; Dawson, P. C.; Freeman, J. L.; Hoy, L. R. J.; Rose, J. B.; Staniland, P. A. *Polymer* **1981**, *22* (8), 1096–1103.
(5) Blundell, D. J.; Osborn, B. N. *Polymer* **1983**, *24* (8), 953–958.
(6) Louden, J. D. *Polym. Commun.* **1986**, *27* (3), 82–84.
(7) Everall, N. J.; Chalmers, J. M.; Ferwerda, R.; Vandermaas, J. H.; Hendra, P. J. *J. Raman Spectrosc.* **1994**, *25* (1), 43–51.
(8) Stuart, B. H. *Spectrochim. Acta, Part A* **1997**, *53* (1), 111–118.
(9) Stuart, B. H. *Tribol. Int.* **1998**, *31* (11), 687–693.
(10) Young, R. J.; Eichhorn, S. J. *Polymer* **2007**, *48* (1), 2–18.
(11) Mitra, V. K.; Risen, W. M.; Baughman, R. H. *J. Chem. Phys.* **1977**, *66* (6), 2731–2736.
(12) Davies, R. J.; Eichhorn, S. J.; Riekel, C.; Young, R. J. *Polymer* **2004**, *45* (22), 7693–7704.
(13) Davies, R. J.; Eichhorn, S. J.; Riekel, C.; Young, R. J. *Polymer* **2005**, *46* (6), 1935–1942.
(14) Davies, R. J.; Montes-Moran, M. A.; Riekel, C.; Young, R. J. *J. Mater. Sci.* **2001**, *36* (13), 3079–3087.
(15) Davies, R. J.; Montes-Moran, M. A.; Riekel, C.; Young, R. J. *J. Mater. Sci.* **2003**, *38* (10), 2105–2115.
(16) Kong, K.; Davies, R. J.; McDonald, M. A.; Young, R. J.; Wilding, M. A.; Ibbett, R. N.; Eichhorn, S. J. *Biomacromolecules* **2007**, *8* (2), 624–630.
(17) Rueda, D. R.; Ania, F.; Richardson, A.; Ward, I. M.; Calleja, F. J. B. *Polym. Commun.* **1983**, *24* (9), 258–260.
(18) Fratini, A. V.; Cross, E. M.; Whitaker, R. B.; Adams, W. W. *Polymer* **1986**, *27* (6), 861–865.
(19) Nishino, T.; Tada, K.; Nakamae, K. *Polymer* **1992**, *33* (4), 736–743.
(20) Voice, A. M.; Bower, D. I.; Ward, I. M. *Polymer* **1993**, *34* (6), 1154–1163.
(21) Hine, P. J.; Ward, I. M.; Olley, R. H.; Bassett, D. C. *J. Mater. Sci.* **1993**, *28* (2), 316–324.
(22) Loos, J.; Schimanski, T.; Hofman, J.; Peijs, T.; Lemstra, P. J. *Polymer* **2001**, *42* (8), 3827–3834.
(23) Alcock, B.; Cabrera, N. O.; Barkoula, N. M.; Wang, Z.; Peijs, T. *Composites, Part B* **2008**, *39* (3), 537–547.
(24) Hine, P. J.; Ward, I. M.; Jordan, N. D.; Olley, R.; Bassett, D. C. *Polymer* **2003**, *44* (4), 1117–1131.
(25) Jordan, N. D.; Bassett, D. C.; Olley, R. H.; Hine, P. J.; Ward, I. M. *Polymer* **2003**, *44* (4), 1133–1143.
(26) Zyex: http://www.zyex.com/index.htm (May **28, 2008**).
(27) Hammersley, A. P. ESRF Internal Report, **1997**; p ESRF97HA02T.
(28) Hammersley, A. P. *Synchrotron Radiat. News* **1989**, *2*, 24.
(29) Northolt, M. G. *Polymer* **1980**, *21* (10), 1199–1204.
(30) Marquardt, D. W. *J. Soc. Ind. Appl. Math.* **1963**, *11* (2), 431–441.
(31) Young, R. J.; Lovell, P. A. *Introduction to Polymers*, 2nd ed.; CRC Press: Boca Raton, FL, 1991.
(32) Agbenyega, J. K.; Ellis, G.; Hendra, P. J.; Maddams, W. F.; Passingham, C.; Willis, H. A.; Chalmers, J. *Spectrochim. Acta, Part A* **1990**, *46* (2), 197–216.
(33) Eichhorn, S. J.; Young, R. J.; Davies, R. J.; Riekel, C. *Polymer* **2003**, *44* (19), 5901–5908.
(34) Moss, C. E.; Butler, M. F.; Muller, M.; Cameron, R. E. *J. Appl. Polym. Sci.* **2002**, *83* (13), 2799–2816.
(35) Brooks, N. W. J.; Unwin, A. P.; Duckett, R. A.; Ward, I. M. *J. Macromol. Sci., Phys.* **1995**, *B34* (1−2), 29–54.
(36) Brooks, N. W.; Duckett, R. A.; Ward, I. M. *Polymer* **1992**, *33* (9), 1872–1880.
(37) Northolt, M. G.; Baltussen, J. J. M.; Schafferskorff, B. *Polymer* **1995**, *36* (18), 3485–3492.
(38) Kong, K.; Eichhorn, S. J. *Polymer* **2005**, *46* (17), 6380–6390.
(39) Eichhorn, S. J.; Sirichaisit, J.; Young, R. J. *J. Mater. Sci.* **2001**, *36* (13), 3129–3135.
(40) Kroonbatenburg, L. M. J.; Kroon, J.; Northolt, M. G. *Polym. Commun.* **1986**, *27* (10), 290–292.
(41) Yeh, W. Y.; Young, R. J. *Polymer* **1999**, *40* (4), 857–870.
(42) Sakurada, I.; Nukushina, Y.; Ito, T. *J. Polym. Sci.* **1962**, *57* (165), 651.

MA801402W